IJCRT.ORG ISSN : 2320-2882

INTERNATIONAL JOURNAL OF CREATIVE RESEARCH THOUGHTS (IJCRT)

An International Open Access, Peer-reviewed, Refereed Journal

Structural, Optical And Morphological Study Of Iodine Doped Zinc Oxide.

Vishal Shukla[1] , Manmohan Mishra[1] , Sandeep Kumar Singh[1] , Prabhuta Sharma[1] , Mahendra Kumar[1]

[1] Nanomaterials and Environmental Sensors Research Lab, Department of Physics, University of Lucknow, Lucknow, India

Abstract – The structural, optical, and morphological characteristics of iodine-doped ZnO thin films produced by the sol-gel spin coating technique are investigated in this work. The films' crystallinity, bandgap, and surface morphology were assessed by XRD, UV-visible spectroscopy, and FESEM at iodine concentrations of 0%, 5%, 10%, and 20%. A hexagonal crystal structure with preferred orientation along the (101) plane and grain sizes ranging from 52 to 65 nm was verified by XRD investigation. SEM pictures showed that there was a xenolith present and that the shape and texture changed with the annealing temperature. The bandgap was calculated to be between 2.80 and 3.45 eV using UV-visible spectroscopy.

Keywords: ZnO, doping, XRD, FESEM, RAMAN, UV-visible

1. Introduction

Zinc oxide (ZnO) is a widely studied semiconductor with promising applications in optoelectronic devices, attributed to its broad bandgap of 3.37 eV and strong exciton binding energy of around 60 meV at room temperature.[1] The impressive chemical and thermal stability of ZnO contributes to its importance in technology. Adjusting its electrical conductivity, bandgap, and charge carrier concentration through selective doping allows for tailored applications in advanced electronics. Research has recently focused on enhancing ZnO's properties by incorporating transition metals such as Mn, Ni, Fe, Co, and Cr. Zinc oxide is widely applied in areas like visible-light photocatalysis, antibacterial treatments, and nanomedicine. Studying iodine-doped ZnO's optical characteristics helps in understanding the impact of dopants on material behavior**.** [2-3] The Photonic and magnetic characteristics of transition metal-doped ZnO have been widely studied. ZnO, known for its broad bandgap, generally functions as an insulator at room temperature but can exhibit conductivity under specific conditions like doping or heating. Its high transparency in the visible spectrum makes it well-suited for various applications. in optical films, coatings, and other light-based technologies. [4–6] Enhancing the electrical and optical capabilities of ZnO is vital for its growing use in advanced technology. It serves an essential role in solar panels, LED technology, antibacterial treatments, and cancer therapy. Its asymmetric structure also improves its efficiency in actuators and piezoelectric transduction applications. [7] Iodine is regarded as one of the most effective dopants for ZnO due to its exceptional stability at zinc sites, making it ideal for enhancing and adjusting its optical and electrical properties.[8] Different fabrication techniques, such as the sol-gel process and chemical vapor deposition, have been used to produce ZnO in doped and undoped forms with varying sizes and structures.[9]

This work focuses on the synthesis of iodine-doped and undoped ZnO thin films using the sol-gel method under carefully controlled temperature and pressure conditions. It presents an in-depth analysis of the films' structural, morphological, compositional, and optical properties, along with details of the fabrication process.

2. **Experimental method :-** In order to deposit the the Spin coating techniques using the sol-gel process was used to create ZnO thin films on glass substrates. As a solvent, starting material and stabilizer, respectively, ethanol (CH_3CH_2OH) 25 ml, distilled water 25 ml and zinc acetate powder (CH_3Co_2) 10 gm were combined, and the mixture was stirred 65 ℃ for 2 h with a 1000 rpm rotation. In given solution dissolved Iodine 0.0, 0.377, 0.756, 1.512 gm, (ie. IZ0, IZ5, IZ10 & IZ20) mixing 15 min with Iodine. Now, just dissolved NaoH (4 Pallets) in given solution then check pH value in that solution (ie. Approx pH =10-12-12-11). Now just repeating stirring given solution 2 h. The resultant was clean homogeneous solution. The glass substrate was cleaned at 90 ℃ for 20 min in methanol, de-ionized water and distilled water. It was then dried in a hot air oven at 100 ℃ for 20 min. The coating solution was dropped onto a glass substrate and spun at 1000 rpm for 1 min by using a spin coater. After the coating process, the films were dried at 250 ℃ for 25 min in a hot air oven in order to evaporate the solvent and remove organic residuals. The procedures from coating were repeated several times until the desired thickness was observed. Finally ZnO film was annealed at 500 ℃ for 3 h in controlled hot temperature Furnace to remove H^+ donors. All the characterization was done immediately after deposition of the thin film.

ZnO thin films were analyzed for their optical properties via UV-Vis spectroscopy (JASCO-670). Structural analysis, along with surface morphology studies covering roughness, boundaries, voids, and defects was performed using the crystallographic structure was analyzed using X-ray diffraction (XRD) with a RIGAKU ULTIMA 4 (Japan), while surface morphology was investigated via SEM using a JOEL JSM-7610F (Tokyo, Japan). To prepare for FESEM imaging, the samples were first dried and then coated with a gold-palladium layer, which enhances conductivity, mitigates charging effects, and ensures better image resolution. optical transmittance measurements were performed using a Renishaw in Via Raman microscope in the 100 - 900 nm wavelength range. UV-Visible absorption spectrum was performed by a spectrometer (JASCO 0670).

3. Characterization techniques

3.1. Structural properties

X-ray diffraction measurements

The structural properties of the samples were examined using X-ray diffraction (XRD) with a Rigaku Ultima IV diffractometer, incorporating a CuKα₁ radiation source (wavelength: 1.5406 Å), as depicted in Fig.1. The XRD patterns indicate that the material is polycrystalline with a hexagonal wurtzite structure. Indexing is obtained Such as (101), (100), (103), (002), (110), (103) and (112). According to XRD analysis, the ZnO thin films exhibit a single-phase structure with a (101) orientation, and no impurity peaks are observed. [10]

To determine the grain size of ZnO particles and assess their crystallinity, diffraction peaks were analyzed using the Scherrer formula. [12,13,14].

$$D = \frac{K\lambda}{\beta \cos\theta} \quad \ldots\ldots\ldots\ldots\ldots\ldots\ldots\ldots (1)$$

Where, D = crystallite size of the particle

K = 0.9 (Scherrer Constant)

λ = 0.15405 nm (Wavelength of light used)

β = FWHM (Full-width half maxima in Radians)

θ = Peak position (radians)

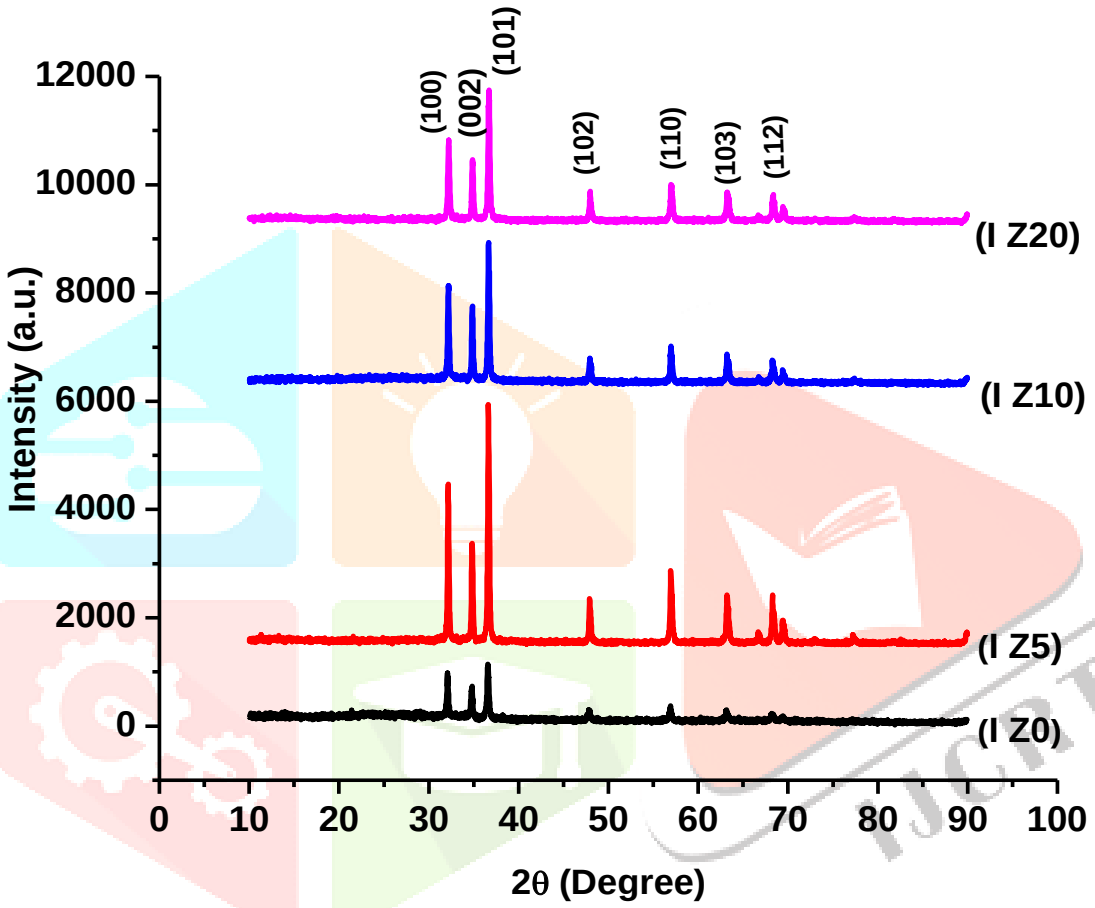

Fig. 1 the XRD spectra of ZnO thin films with varying iodine concentrations, annealed at 500°C.

The dislocation density is computed using the specified equation. [15]

$$\delta = \frac{1}{D^2} \quad \text{..... (2)}$$

The parameters a, b, and c, which describe a hexagonal crystal structure, are calculated using suitable mathematical expressions.

$$\frac{1}{d^2_{(hkl)}} = \frac{4}{3}\left(\frac{h^2+hk+k^2}{a^2}\right) + \frac{l^2}{c^2} \quad \text{..... (3)}$$

The interplanar distance, dhkl, is related to the Miller indices h, k, and l, which are essential for determining the geometry of a crystal. The unit cell volume, 'V', for each of the four samples was then calculated based on a formula that takes these factors into account, ensuring accurate representation of the crystal structure.

$$V = \sqrt{\frac{3}{2}}\, a^2 c \qquad \ldots\ldots\ldots\ldots\ldots\ldots (4)$$

Table 1 Showing average crystallite size (D), lattice parameter, Volume (V), average dislocation density (δ) of different peaks.

Iodine Doping (%)	Avg. D (n m)	δ (nm^{-2})	δ×10^{-4} (nm^{-2})	Lattice Parameter (Å)			
				a = b	c	$\frac{c}{a}$	V
IZ0	55.61	3.092×10^{-4}	3.092	3.204	5.16	1.610	45.869
IZ5	65.09	4.236×10^{-4}	4.236	3.206	5.152	1.606	45.856
IZ10	64.83	4.202×10^{-4}	4.202	3.030	4.996	1.648	39.721
IZ20	52.97	2.805×10^{-4}	2.805	3.201	5.146	1.607	45.660

The crystallographic constants of ZnO thin films undergo changes due to iodine doping. wat 5% iodine doping were a = b = 3.206 Å and c = 5.152 Å, in agreement with earlier reports With increasing iodine concentration, the lattice parameters decreased, and crystallite size initially increased up to 10%, but decreased again at 20 % doping.

3.2. Morphological studies

Scanning electron microscopy (SEM)

The shape and size of ZnO nanoparticles were analyzed using Field Emission Scanning Electron Microscopy (FESEM) images of iodine-doped samples, as shown in Fig.2.

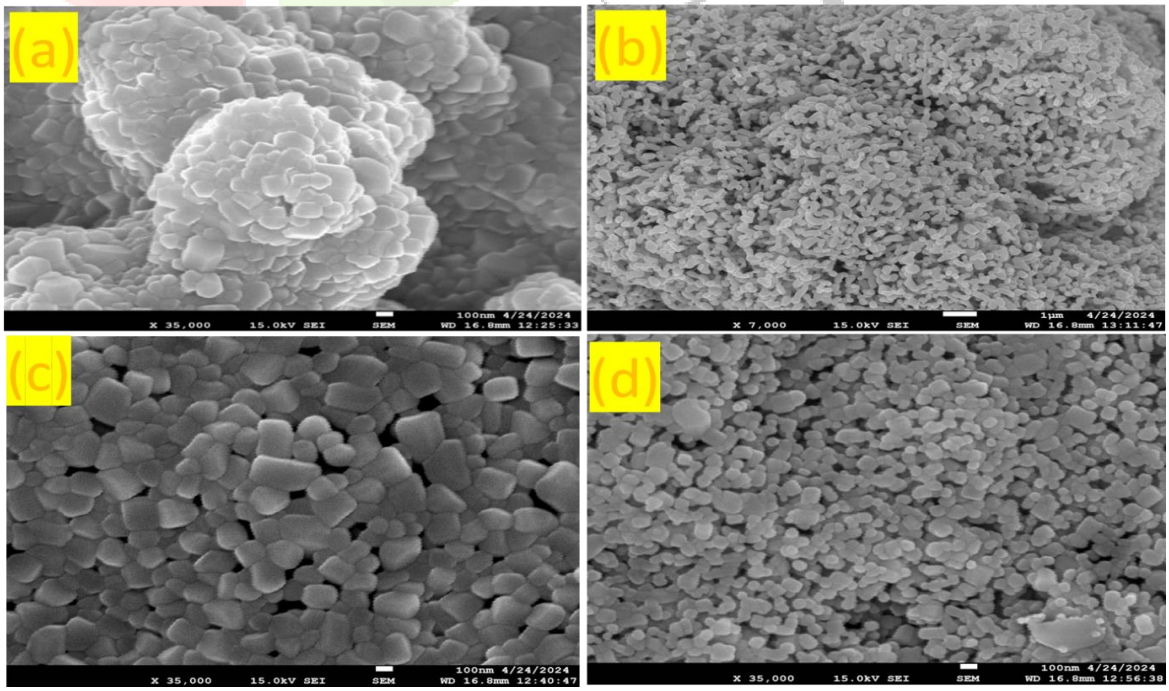

Fig. 2 Showing for different doping percentage (a) Pure ZnO (b, c & d) 5,10 & 20 % Iodine doped ZnO

after annealing at 500°C. The scanning electron microscope (JOEL JSM 7610f, Tokyo, Japan) functioned under a 5 kV acceleration voltage during operation. According to SEM analysis, a gold-palladium coating was applied to the sample holder to reduce particle charging. FESEM images demonstrated that increasing the annealing temperature led to larger ZnO particles, as higher thermal energy enhanced atomic mobility and improved crystallinity.

3.3 Raman Spectroscopy :- The crystal structure of pure and Iodine-doped ZnO materials is further Investigated by Raman spectroscopy. The Raman spectra of pure and Iodine-doped bulk materials recorded at seen temperature and are shown in fig.3 optical transmittance measurements were performed using a Renishaw in Via Raman microscope in the 100 - 900 nm wavelength range.

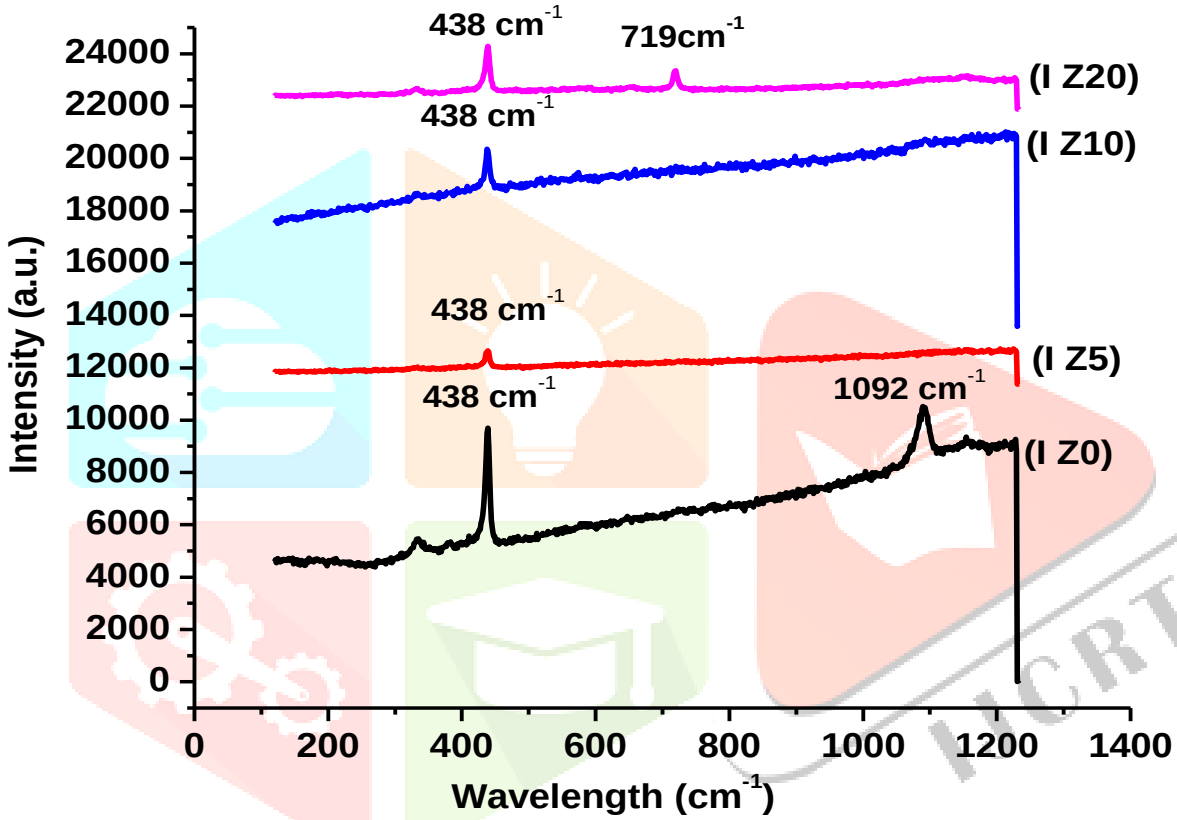

Fig.3 Raman Spectroscopy annealing at 500 ℃

The Raman spectrum of ZnO exhibits optical phonon modes within the 200–1200 cm^{-1} range. A distinct band at 438 cm^{-1} appears in the lower wavenumber region, corresponding to the transverse optical (TO) phonons of the A_1 and E_1 modes. The A_1 mode is linked to structural defects, including iodine vacancies and interstitial zinc atoms. Additionally, the characteristic 719 cm^{-1} peak, which signifies the wurtzite structure of ZnO, represents the E2 (high) mode and is highly responsive to crystallinity and material defects.[16] The Raman peak observed at 580 cm^{-1} is associated with the E1 (LO) vibrational mode. In pure ZnO, a distinct and intense peak appears at 438 cm^{-1}, which corresponds to the E_2 (high) mode. a characteristic indicator of the wurtzite crystal structure. For the iodine-doped samples (10% and 20%), additional peaks in the 1000–1200 cm^{-1} region were detected, which could be indicative of an impurity phase due to iodine.[17]

3.4. Optical properties

UV–visible Spectroscopy :-

After aging, the transmittance spectra of ZnO thin films subjected to different annealing temperatures are displayed in Fig.4 as a function of photon wavelength. Measurements were taken using a UV– vis spectrometer (JASCO 0670). As the annealing temperature increases, the ZnO films exhibit higher transmittance, which can be attributed to enhanced crystallinity and a reduction in structural defects. An anomaly is observed at 500°C, possibly due to the 3-hour annealing process causing the glass substrate to distort. We find that bandgap first increases to 3.45 eV at 5 % Iodine doping in ZnO whereas after increase in doping level bandgap decreases again.

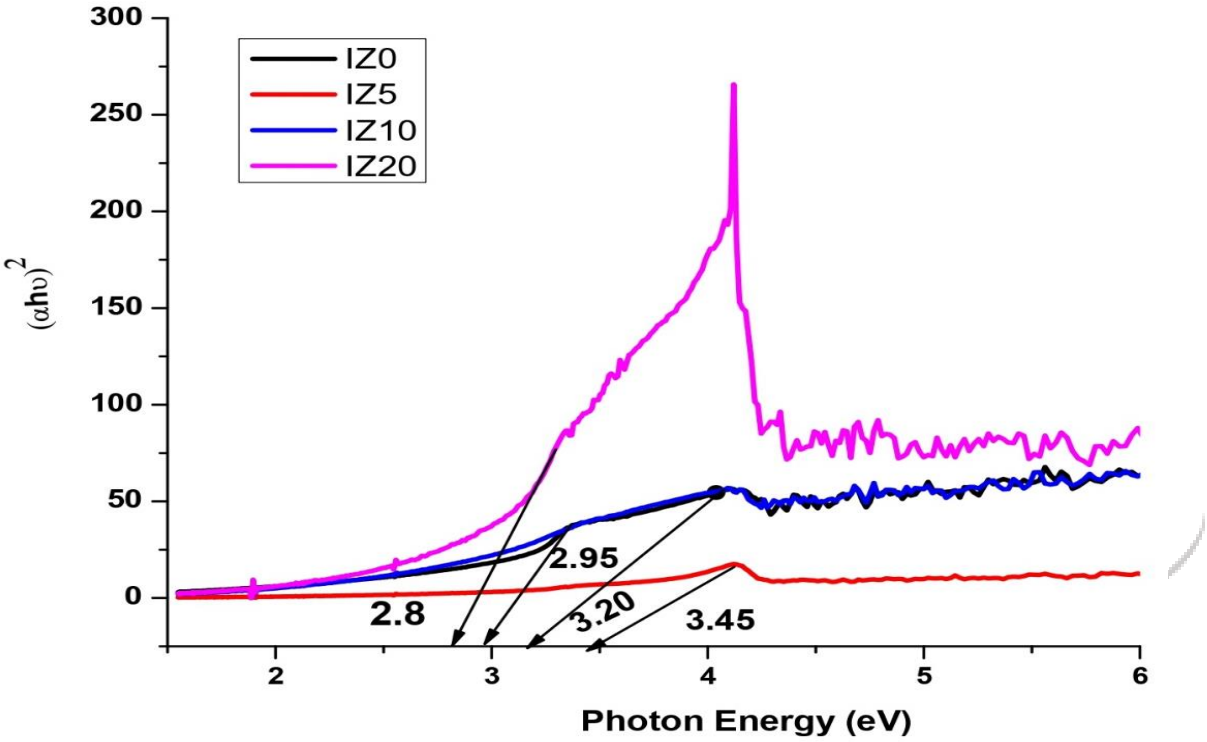

Fig.4 showing optical band gap at 500 ℃

Doping %	Bandgap
0	2.95 eV
5	3.45 eV
10	3.20 eV
20	2.80 eV

Table 2 optical band gap at different doping concentrations

The optical absorption spectra of Iodine-doped ZnO nanoparticles milled for 3 hours were recorded in the 300–800 nm range to assess the optical characteristics. Doping introduced shallow energy states in the band gap, causing a red shift in the UV-visible absorption edge. [10-11]

4. **Conclusion -** In this study, undoped and iodine-doped ZnO nanoparticles were developed via the sol-gel spin coating method. Upon annealing at 500°C for three hours, the ZnO thin film revealed a hexagonal phase with grain dimensions ranging from 52 to 65 nm. The computed dislocation density was 1.6020, while the lattice constants were a = b = 3.1602 Å and c = 5.1135 Å, confirming a nanostructured formation. The estimated bandgap ranged between 2.80 and 3.45 eV.

Data availability

Access to the data can be granted upon request.

Acknowledgment

Lab facilities provided by the Nanomaterials & Environmental Sensors Research Laboratory, Department of Physics, University of Lucknow, also providing XRD, UV-Visible and BSIP Lucknow, providing FE-SEM, RAMAN by BHU providing lab facilities.The Manmohan Mishra is grateful for the financial assistance provided by the FELLOWSHIP NO- 201610047204, a CSIR-UGC JRF fellowship.

References

1. G. Srinet, Ravindra Kumar*, V. Sajal (2013) Effects of Ni doping on structural, optical and dielectric properties of ZnO Ceramics International 39 (2013) 7557–7561.

2. B.K. Das and T. Das, K. Parashar, S.K.S. Parashar (2017) Structural, optical and dielectric study of Cu doped ZnO nanoparticles synthesised by high energy ball milling Int. J. Nano and Biomaterials, Vol.7, No. 2.

3. Mishra, Manmohan, Vishwas Pratap Banga, Mahendra Kumar, and Monu Gupta. "Effect of aging on transmittance, and effect of annealing temperature on CO2 sensing of ZnO thin film deposited by spin coating." *e-Prime-Advances in Electrical Engineering, Electronics and Energy* 7 (2024): 100405.

4. Mishra, Manmohan, and Mahendra Kumar. "Elevating energy storage: High-entropy materials take center stage." *Journal of Energy Storage* 91 (2024): 112186.

5. Mishra, Manmohan, and Mahendra Kumar. "Effects of Al doping on structural, optical, morphological, and low-concentration CO2 gas sensing properties of ZnO nanoparticles synthesized by sol-gel method." *Physica Scripta* 99, no. 12 (2024): 125929.

6. Mishra, Manmohan, Sandeep Kumar Singh, and Mahendra Kumar. "Annealing Temperature Effects on Sno2 Thin Films: Structural, Optical, Morphological, and Electrical Properties for Optoelectronics." *Optical, Morphological, and Electrical Properties for Optoelectronics*.

7. C.K. Ghosh, S. Malkhandi, M.K. Mitra, K.K. Chattopadhyay, Effect of Ni doping on the dielectric constant of ZnO and its frequency dependent exchange interaction, Journal of Physics D: Applied Physics 41 (2008) 245113

8. Mishra, Manmohan, Mahendra Kumar, Vikram Soni, and Atul Srivastava. "13. Unveiling the Nanoscale: A Journey through Scanning Electron Microscopy (SEM)." *THE SYMPHONY OF KNOWLEDGE* (2023): 222.

9. M. Mishra, V.P. Banga, M.K., M.G. Effect of aging on transmittance, and effect of annealing temperature on CO_2 sensing of ZnO thin film deposited by spin coating. Advances in Electrical Engineering, Electronics and Energy 7 (2024) 100405.

10. Saw, K.G., Aznan, N.M., Yam, F.K., Ng, S.S. and Pung, S.Y. (2015) 'New insights on the Burstein-Moss shift and band gap narrowing in indium-doped zinc oxide thin films', PLoS ONE, Vol. 10, No. 10 p.0141180.

11. C. Suryanarayana, M.G. Norton, X-ray Diffraction: A Practical Approach, Plenum Press, New York, 1998.

12. A.Shah · M. Ahmad· Rahmanuddin · Shakil Khan, The role of Al doping on ZnO nanowire evolution and optical band gap tuning, Applied Physics A (2019) 125:713

13. S. Maniv, A. Zangvil, Controlled texture of reactively rf-sputtered ZnO thin films, J. Appl. Phys. 47 (1978) 2787–2792.

14. W. Muhammad, S. Ullah, M. Haroon, B. Abbasi, Optical, morphological and biological analysis of zinc oxide nanoparticles (ZnO NPs) using Papaver somniferum L, RSC Adv. 9 (2019) 29541–29548.

15. Manoj K. Gupta, Binay Kumar∗ Enhanced ferroelectric, dielectric and optical behavior in Li-doped ZnO nanorods,Journal of Alloys and Compounds 509 (2011) L208–L212

16. J.B. Wang, G.J. Huang, X.L. Zhong, L.Z. Sun, Y.C. Zhou, Appl. Phys. Lett. 88, 252502 (2006)

17. R. Joshi, P. Kumar, A. Gaur, K. Asokan, Appl. Nanosci. 4, 531 (2014